Cancer Chemother Pharmacol (2011) 67:369–379
DOI 10.1007/s00280-010-1335-8

ORIGINAL ARTICLE

Chemotherapeutic activity of silymarin combined with doxorubicin or paclitaxel in sensitive and multidrug-resistant colon cancer cells

Valentina Colombo · Monica Lupi · Francesca Falcetta · Daniele Forestieri · Maurizio D'Incalci · Paolo Ubezio

Received: 29 January 2010 / Accepted: 14 April 2010 / Published online: 30 April 2010

Abstract
Purpose The milk thistle extract silymarin, alone or in combined chemotherapy, is now under investigation in anticancer research, with particular interest for its possible employ in the treatment of chemoresistant tumours. So far, the consequences of a silymarin pre-treatment have not been thoroughly investigated. We studied whether silymarin pre-treatment synergized with chemotherapy, exploring the dose-dependence of the interaction in sensitive and multidrug-resistant cells.
Methods We studied cell cycle perturbations induced by silymarin in two colon carcinoma cell lines, LoVo and the multidrug-resistant isogenic LoVo/DX. Synergism/additivity/antagonism of silymarin–doxorubicin silymarin–paclitaxel combined treatments were evaluated by isobologram/combination index analysis, in the whole spectrum of active and sub-active concentrations of all drugs. The mechanisms of silymarin interaction with the other drugs were investigated by measuring drug uptake and cell cycle perturbations.
Results Silymarin had similar antiproliferative activity against both cell lines. Pre-treatment with low silymarin concentrations synergised with both doxorubicin and paclitaxel in LoVo but not in LoVo/DX. Higher silymarin concentrations were additive with doxorubicin and paclitaxel in both cell lines. Silymarin favourably interfered with uptake and cell cycle effects of the chemotherapeutics in LoVo but not in LoVo/DX.
Conclusion These findings confirm activity of silymarin against colon carcinoma, including multidrug-resistant types, at relatively high but clinically achievable concentrations. In view of its low toxicity, two schedules based on low- and high-dose silymarin pre-treatment might offer a valuable option for combined treatment.

Keywords Silymarin · Combination chemotherapy · Synergism · Multidrug resistance · Drug uptake · Flow cytometry

V. Colombo · M. Lupi · F. Falcetta · D. Forestieri · M. D'Incalci · P. Ubezio (✉)
Laboratory of Anticancer Pharmacology,
Department of Oncology, Istituto di Ricerche Farmacologiche "Mario Negri", Via La Masa 19, 20156 Milan, Italy
e-mail: paolo.ubezio@marionegri.it

Introduction

It is known that the antitumour activity of anticancer drugs can be enhanced by combining them with modulating agents to reduce their toxicity and/or boost their antitumour activity [5]. This is particularly important considering that many human tumours have resistance mechanisms responsible for the failure of chemotherapeutic treatment, so the use of resistance-counteracting compounds is potentially useful. The milk thistle extract silymarin, commonly used for its hepatoprotective [12] and antioxidant [13, 25] properties, is under study in cancer research both as a chemopreventive and as a modulating compound. Silymarin is a mixture of flavonolignans, mainly silibinin (also named silybin, with two diasteroisomers silybin A and silybin B), isosilybin (with two diasteroisomers isosilybin A and isosilybin B), silydianin and silychristin, among which silibinin is the most active, but not the only active constituent [24]. Preclinical studies indicate that silymarin or silibinin counteract carcinogenesis in models of prostate, lung, colon, ovarian and non-melanoma skin cancer [21]. The use of silymarin is also favoured by its tolerability, which permits prolonged oral

treatment with no limiting side-effects, even in patients with cancer [20].

On the other side, the drug-modulating effect of silymarin was demonstrated by its ability to potentiate the cytotoxic effect of doxorubicin or cisplatin against breast and prostate cancer cells [7, 37, 38]. Further studies suggest that this effect is at least partly due to silymarin influencing on the active transport of drugs through the cell membrane, acting particularly on mechanisms that cause multidrug resistance, increasing drug efflux by over-expression of ATP-binding cassette (ABC) transporters such as MDR1 P-glycoprotein (P-gp, ABCB1) and multidrug resistance-associated protein 1 (MRP1, ABCC1) [3, 30]. Therefore, silymarin-based therapies might be particularly useful in the management of multidrug-resistant tumours.

Previous studies have investigated the activity of silymarin in colon cancer cells [1, 22, 33] but its activity against multidrug-resistant cells and drug combinations have not been evaluated. The present study was undertaken to test the antitumour activity of silymarin alone and in combination against colon cancer cells, in a cell line sensitive to doxorubicin (LoVo) and its multidrug-resistant (MDR) isogenic counterpart (LoVo/DX). Silymarin was tested in combination with doxorubicin and paclitaxel at a wide concentration range of drugs, allowing a thorough analysis of potential synergism or antagonism. We also compared drug uptake/efflux and cell cycle perturbations in the two cell lines in the presence or absence of silymarin, to clarify the putative contribution of these phenomena to the effect of the combination.

Materials and methods

Drugs and chemicals

Silymarin (Legalon®) (SIL) was kindly provided by Madaus srl, Padova, Italy. The preparation contains 75.0–80.9% silymarin, including silibinin (26–31% in weight), isosilybin (10–14%), silychristin (12–14%). Silydianin (14–17%) [8].

Paclitaxel (Taxol®) (TAX) was provided by Indena S.p.A., Milan, Italy, doxorubicin (DOX) by Nerviano Medical Sciences, Nerviano, Italy.

Cell culture

A human colon adenocarcinoma cell line (LoVo), isolated from a metastatic nodule, and its MDR variant (LoVo/DX) were used. Both cell lines were grown as previously described [9]. The LoVo/DX cell line was selected for resistance to DOX from its drug-sensitive parental LoVo cell line [17] and was also resistant to other anthracyclines, to vinca alkaloids and epipodophyllotoxin derivatives [9]. LoVo/DX cells have high levels of expression of P-gp [9, 29].

Detection of doxorubicin and paclitaxel by high-performance liquid chromatography (HPLC)

Doxorubicin and paclitaxel were determined in cell pellets by using two previously reported HPLC methods after solvent or solid phase extraction, respectively [4, 41].

Flow cytometric detection of doxorubicin

The inherent fluorescence of DOX can be combined with flow cytometry as a convenient and rapid method for the quantification of DOX uptake and efflux [10, 23]. There is a good correlation between the average cellular fluorescence intensity and the amount of drug associated with the cells as detected by HPLC. DOX fluorescence was analysed using a FACSCalibur flow cytometer (Becton–Dickinson Immunocytometry Systems, Inc., San Jose, CA) with excitation at 488 nm and emission in the 562–606 nm range. Dead cells were excluded on the basis of their scatter signal and propidium iodide (PI) stainability.

Cell cycle perturbations and apoptosis

Exponentially growing cells were treated with different drug concentrations in T-25 cm^2 tissue culture flasks (Iwaki, Bibby Sterilin, Staffordshire, UK). After treatment, the cells were washed twice with warm PBS and left in drug-free medium for the specified times. At each time, the cells were detached, counted, fixed and prepared for cytometric DNA and TdT-mediated dUTP nick end labelling (TUNEL) analyses as described before [28]. DNA histograms were analysed using a previously described software [39] obtaining the percentage of cells in the cell cycle phases (%G_1, %S, %G_2M).

Combination treatment

To evaluate the effect of the combination of SIL and DOX (or TAX), cells were treated, left in drug-free medium up to 7 days and tested with sulphorodamine B (SRB) [2]. A factorial experimental design was adopted in each experiment, where single concentrations of SIL were coupled with several concentrations of DOX (or TAX) and vice versa, in 96-well plates, with five replicated independent plates. Several concentrations were considered for each drug: SIL concentrations were in the range 1–100 μg/ml in both cell lines, DOX in the range 3–50 nM (LoVo) and 40–3,000 nM (LoVo/DX), TAX in the range 0.4–40 nM (LoVo) and

100–2,000 nM (LoVo/DX). Each schedule was tested in at least two independent experiments.

Data were first analysed using the isobologram method, relying on fitting of the combined concentrations of SIL and DOX (or TAX) that caused a growth inhibition of 30, 50 or 70% (reviewed in [18]).

To quantify the interaction, we calculated the combination index (CI) for each pair of drug concentrations tested in combination (D_{sil}, D_{dox}), with the following formula (based on the Lowe additivity criterion [27]):

$$CI = D_{sil}/IC_{X,sil} + D_{dox}/IC_{X,dox}$$

where X is the observed effect in the combination, $IC_{X,sil}$ and $IC_{X,dox}$ are the concentrations of each individual drug that would produce the same effect "X" if given alone.

Interaction was claimed additive if $0.85 < CI < 1.15$, synergistic if $CI \leq 0.85$, antagonistic if $CI \geq 1.15$. To support the claim with a statistical test, SIL and DOX (or TAX) concentrations were grouped on the basis of the effect of the single drug in the "low-efficacy" (growth inhibition between 5 and 30%) and "high-efficacy" (growth inhibition between 30 and 70%) groups. SIL concentrations that were almost ineffective (less than 5% growth inhibition) but higher than 0.5 μg/ml were considered as an additional "sub-efficacy" group. "Sub-effective" concentrations of DOX and TAX were not evaluated.

Eventually, all the combination data of at least two repeated experiments with a given cell line entered the analysis, and the results were pooled in the following six groups: (SIL_{sub}, DOX_{low}), (SIL_{sub}, DOX_{high}), (SIL_{low}, DOX_{low}), (SIL_{low}, DOX_{high}), (SIL_{high}, DOX_{low}), (SIL_{high}, DOX_{high}).

Means and the standard deviation of the CI in each group were calculated. The significance of the difference of the mean from a given CI was evaluated using a two-sided *t* test. Synergy was significant if average CIs were lower than 0.85 and statistically different from 1; antagonism if they were higher than 1.15 and statistically different from 1; additivity if they were between 0.85 and 1.15, significantly higher than 0.8 and lower than 1.2.

Results

Antiproliferative activity of silymarin in LoVo and LoVo/DX

Silymarin was tested in a human colon adenocarcinoma cell line (LoVo), isolated from a metastatic nodule, and its MDR variant (LoVo/DX). The characterisation of the MDR phenotype of LoVo/DX cells has been reported elsewhere, particularly evidencing a 2-log increase in the expression of P-gp [29]. In our experiments with the SRB test, LoVo/DX cells were about 72 times less sensitive to DOX than LoVo (IC50 892 and 12 nM, respectively, as average of at least three independent experiments) and 78 times less sensitive to TAX (IC50 1,112 and 14 nM). Instead, LoVo/DX cells were only slightly less sensitive to SIL than LoVo (IC50 70 and 51 μg/ml) (not shown).

The time-course of the antiproliferative effects of SIL was investigated by contemporaneous absolute cell count and DNA flow cytometry. Cells were treated for 24 h with different SIL concentrations and then analysed for additional 48 h.

Treatment with 10 μg/ml SIL induced only a weak, reversible delay in LoVo cells (Fig. 1a), with a small non-significant increase in the percentage of cells in G_2M phase (particularly at 48 h, Fig. 1b), while the same concentration was ineffective in LoVo/DX. At 50 μg/ml, cell proliferation was strongly reduced during SIL treatment, in association with increased percentage of cells in G_1 (Fig. 1b, 24 h panels). The increased $\%G_1$ was observed also at 100 μg/ml in LoVo/DX, while this effect was less evident in LoVo, indicating that growth arrest (Fig. 1a) was not specific for a particular phase. After drug wash-out, we observed an increase in $\%G_2M$ in LoVo, (Fig. 1b, 48 h), reaching the relatively highest value in samples treated with 100 μg/ml. Taken together with the persistent growth inhibition (Fig. 1a, 48 h), the data indicated that in the first day after 100 μg/ml SIL treatment LoVo cells moved slowly through G_1 and S phases but then were arrested in G_2M. At 72 h, proliferation was resumed and G_2M block was resolved, while controls and samples treated with lower concentrations were approaching confluence increasing the percentage of G_1 due to the presence of quiescent/G_0 cells. Proliferation was resumed earlier in LoVo/DX, where a frank increase in cell number was observed in the second day, particularly with 50 μg/ml SIL (Fig. 1b).

Apoptosis over control levels (2% apoptotic cells, as detected by the TUNEL assay) was not observed up to 50 μg/ml SIL in both cell lines. SIL at a concentration of 100 μg/ml induced apoptosis modestly, with a maximum of 10% apoptotic cells reached at 48 h in LoVo and at 24 h in LoVo/DX (not shown).

Synergism, additivity and antagonism of combinations of silymarin with doxorubicin or paclitaxel

The antiproliferative effect of combined SIL-DOX and SIL-TAX treatments were evaluated in experiments challenging several combinations with drug concentrations spanning the whole efficacy range in LoVo and LoVo/DX cells. At least two drug interaction experiments were done for each schedule and drug combination. We used the isobologram analysis [18] for qualitative assessment of synergy or antagonism. The normalised concentrations of

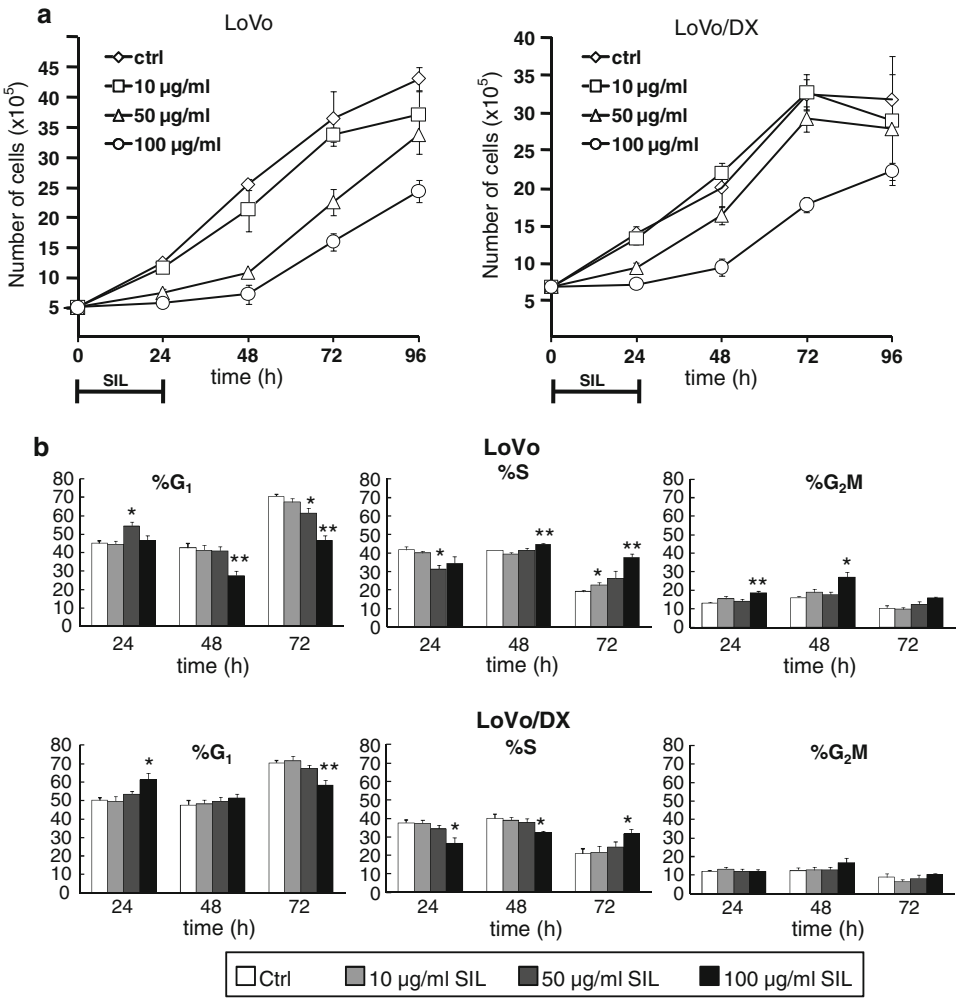

Fig. 1 Time– and dose–responses of the antiproliferative effect of SIL. LoVo and LoVo/DX cells were treated for 24 h with 10, 50 or 100 µg/ml SIL, counted and fixed for flow cytometric analyses at the indicated times from the start of treatment. **a** Absolute cell count. **b** Cell cycle percentages obtained by DNA flow cytometry. Data points and error bars represent the mean and standard error of three replicate samples. *Asterisks* mark values significantly different from relevant controls ($*P < 0.05$, $**P < 0.01$, two-tailed t test)

the combinations causing 30, 50 or 70% growth inhibition could be evaluated by their position in relation to the line of additivity, connecting all pairs of drug concentrations expected to produce 30, 50 or 70% growth inhibition. In order to potentiate the possible interaction of SIL with the second drug, SIL treatment started 24 h before addition of the second drug. When 24 h SIL was followed by 24-h co-treatment with DOX, synergism was detected at all efficacy levels in LoVo, with most data points below the additivity line (Fig. 2a). Instead, combinations data were near the additivity line or above it in LoVo/DX, depending on concentration range (Fig. 2b). Similarly, 24-h SIL-TAX co-treatments were frankly synergistic in LoVo (Fig. 3a) and additive/antagonistic in LoVo/DX cells (Fig. 3b).

In order to quantify the interaction and objectively to test the significance of synergism/additivity/antagonism at different concentration ranges, we calculated the CI for each pair of drug concentrations, grouping the values obtained with concentrations of low or high efficacy of each drug, as defined in the Methods section. In LoVo cells (Table 1a, c), in the "low-efficacy" SIL group, including concentrations around 10 µg/ml, producing 5–30% growth inhibition as single treatment, average CIs were near 0.5. The synergism was highly significant ($P < 0.0001$) for both low and high concentrations of DOX and TAX. These moderately effective SIL concentrations were the most efficient to synergize with DOX and TAX. Lower SIL concentrations, in the "sub-efficacy" group, around 1 µg/ml, producing less than 5% growth inhibition as single treatment, were generally only additive, with a possible (not significant) synergism only observable when combined with low DOX concentrations.

SIL concentrations in the "high-efficacy" group, 30–50 µg/ml, producing 30–70% growth inhibition as single treatment, synergized with "high-efficacy" DOX and "low-efficacy" TAX concentrations, but were additive otherwise.

In LoVo/DX cells, no synergism was found. Both SIL-DOX and SIL-TAX combinations (Table 1b, d) were antagonistic at sub-effective SIL concentrations, additive/

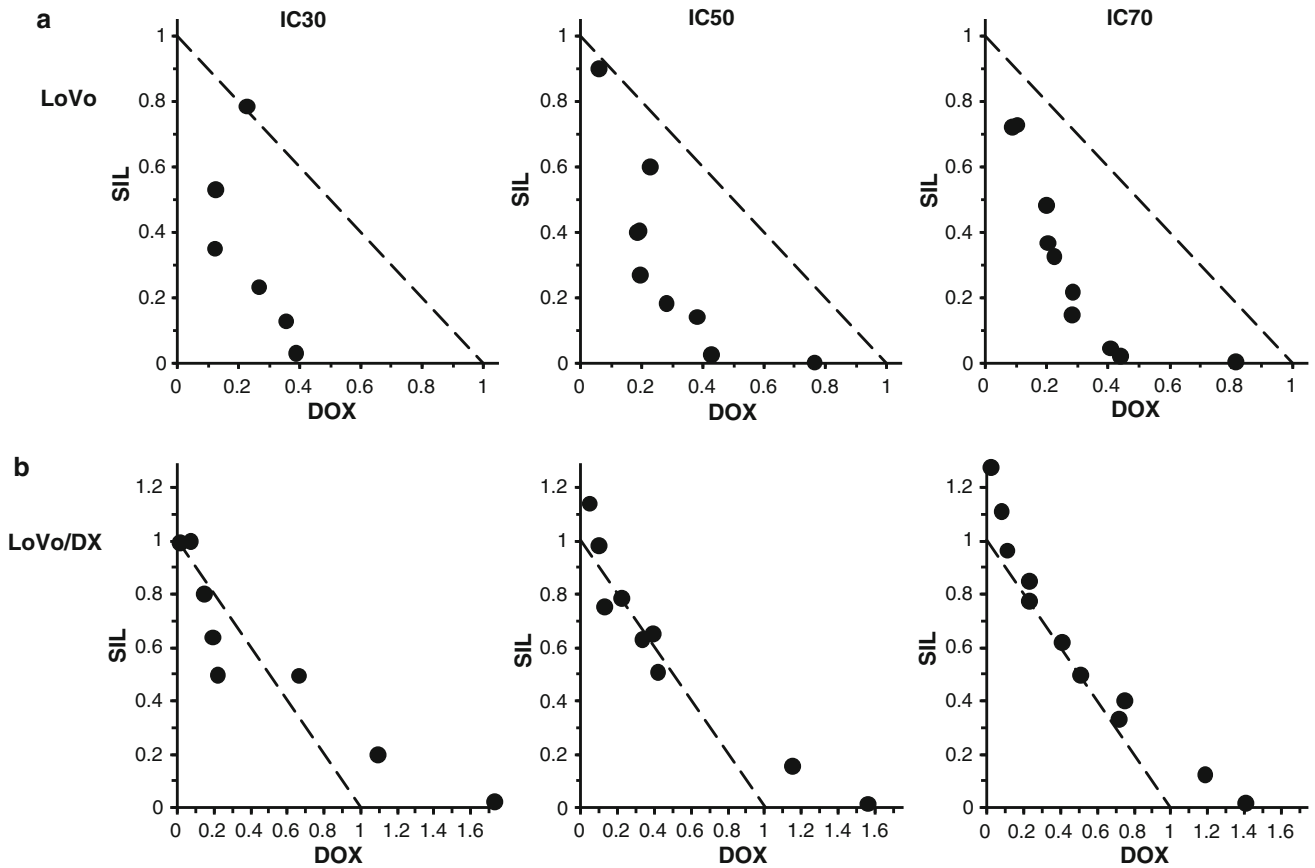

Fig. 2 Isobolograms of SIL-DOX combinations in LoVo (**a**) and LoVo/DX cells (**b**) at the IC30, IC50 and IC70 levels. SIL was given for 24 h alone, then DOX was added for another 24 h. Cell cultures were tested with SRB after 7 days. Abscissa: DOX concentration, as a fraction of DOX IC30, IC50 or IC70; ordinate: SIL concentration, as a fraction of SIL IC30, IC50 or IC70. The additivity line (*dashed*) separates the antagonistic (*upper*) from the synergistic (*lower*) region. The cells were exposed to a range of concentrations of SIL plus DOX. Combined concentrations producing 30, 50 and 70% growth inhibition were calculated by fitting dose–response curves of SIL at each tested DOX concentration and viceversa

slightly antagonistic at low SIL concentrations and additive at high SIL concentrations.

Doxorubicin and paclitaxel cellular uptake and its modulation by silymarin

In order to disclose the cellular mechanism of the observed synergism, we have investigated whether SIL interfered with DOX and TAX uptake. To this purpose, cells were pre-treated with SIL for 24 h then DOX or TAX was added for another 24 h. At the end of the treatment, cells were harvested, counted, centrifuged and DOX or TAX measured in the pellet using HPLC. We found that intracellular drug content of both DOX and TAX was enhanced by SIL (Fig. 4). However, 1 μg/ml SIL was ineffective and at least 10 μg/ml SIL was required to produce the effect, which was higher for DOX than for TAX. Aliquots of the same samples were re-suspended in drug-free medium for evaluation of the efflux. Efflux, evaluated by residual intracellular drug content 30 min after drug wash-out, was not affected by SIL, remaining fast in LoVO/DX and slow in LoVo irrespective of SIL treatment.

Exploiting the intrinsic DOX fluorescence, DOX uptake was also evaluated on a cell-by-cell basis by flow cytometry, with the additional feature of excluding dead and dying cells by counter-stain with propidium iodide. Using the same treatment protocol, intracellular DOX fluorescence was measured at the end of treatment and 30 min after drug wash-out (Fig. 4c). The results confirmed the HPLC measure, demonstrating that DOX fluorescence at the end of treatment was significantly higher in samples treated with 10 μg/ml SIL with respect to cells without SIL. At lower concentrations, SIL was almost ineffective, while 50 μg/ml led to higher DOX accumulation. The effect was stronger in LoVo than in LoVo/DX cells. The efflux of DOX from LoVo/DX cells was rapid, leaving about 8% of the original fluorescence signal at 30 min in SIL-untreated samples, and equally rapid in cells treated with SIL. Instead, more than 50% of the DOX intracellular content at the end of treatment was still inside LoVo cells

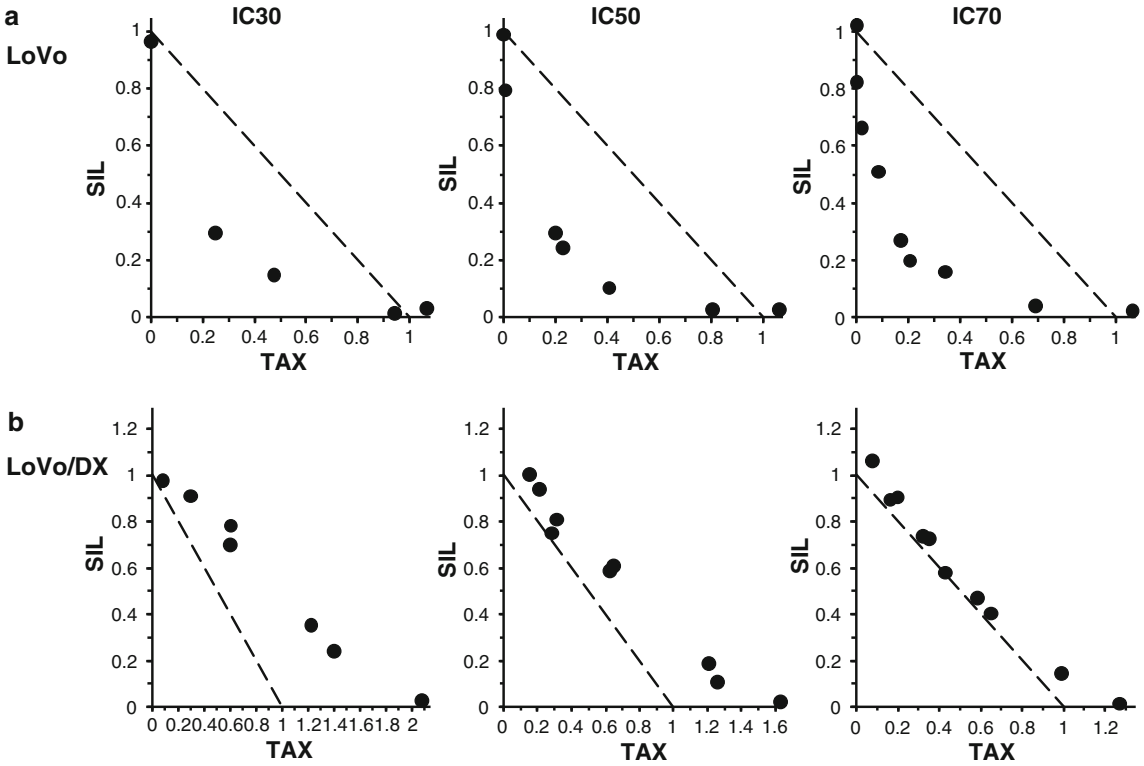

Fig. 3 Isobolograms of SIL-TAX combinations in LoVo (**a**) and LoVo/DX (**b**). SIL was given for 24 h, then paclitaxel was added for 24 h. Abscissa: TAX concentration, as a fraction of TAX IC30, IC50 or IC70; ordinate: SIL concentration, as a fraction of SIL IC30, IC50 or IC70. See Fig. 2 for explanation of isobolograms

Table 1 Combination indexes (CI) of drug interactions in different concentration ranges

DOX conc	SIL concentration		
	Sub-efficacy	Low efficacy	High efficacy
(a) LoVo			
Low efficacy	0.67 ± 0.22 SYN	0.57 ± 0.05 SYN**	0.9 ± 0.11 ADD
High efficacy	0.87 ± 0.19 ADD	0.44 ± 0.03 SYN**	0.66 ± 0.06 SYN**
(b) LoVo/DX			
Low efficacy	1.73 ± 0.23 ANT*	1.19 ± 0.07 ANT**	1.04 ± 0.03 ADD**
High efficacy	1.37 ± 0.1 ANT**	1.20 ± 0.15 ANT	1.09 ± 0.04 ADD*
TAX concentration	SIL concentration		
	Sub-efficacy	Low efficacy	High efficacy
(c) LoVo			
Low efficacy	1.10 ± 0.01 ADD**	0.51 ± 0.05 SYN**	0.83 ± 0.05 SYN**
High efficacy	1.06 ± 0.04 ADD*	0.50 ± 0.07 SYN**	1.06 ± 0.11 ADD
(d) LoVo/DX			
Low efficacy	1.64 ± 0.39 ANT	1.22 ± 0.09 ANT*	1.07 ± 0.03 ADD**
High efficacy	1.77 ± 0.27 ANT**	0.98 ± 0.06 ADD**	1.03 ± 0.04 ADD**

a: SIL-DOX combination in LoVo cells; b: SIL-DOX in LoVo/DX; c: SIL-TAX in LoVo; d: SIL-TAX in LoVo/DX. Mean and standard error of the CI in each concentration range are indicated in each box of the table. See text for definition of the "sub-efficacy", "low-efficacy" and "high-efficacy" concentration ranges. Synergism (SYN) was claimed for mean CI of <0.85, antagonism (ANT) for CI of >1.15, additivity (ADD) elsewhere. Asterisks indicate that CI are significantly different from 1, in the cases of synergism and antagonism, and significantly different from 0.8 and 1.2 for additivity (*t* test, * $P < 0.05$, ** $P < 0.01$)

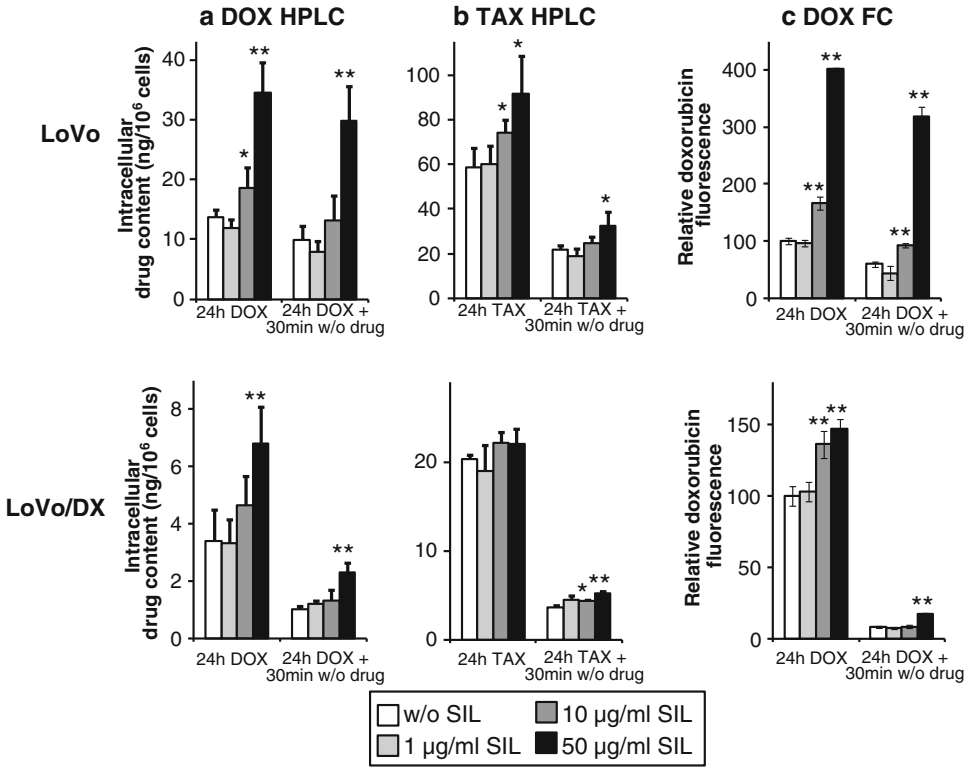

Fig. 4 Intracellular content of DOX and TAX in the presence of SIL. Samples were pre-treated for 24 h with 1, 10 or 50 µg/ml SIL or not pre-treated and then treated with either DOX (0.2 µM) or TAX (0.5 µM) for 24 h. Intracellular DOX or TAX content was measured at the end of treatment and 30 min later by HPLC (**a** and **b**). Effect of SIL on DOX uptake and efflux measured by flow cytometry (**c**). After SIL pre-treatment, 0.15 µM (LoVo) or 1.5 µM (LoVo/DX) DOX was added. After 24 h, cells were detached and intracellular DOX fluorescence was measured by flow cytometry. Cells were washed, suspended in drug-free medium and re-analysed 30 min later. Average DOX fluorescence was normalised to the fluorescence of controls with DOX without SIL at the end of treatment in the same cell line. Column height and error bars represent the mean and standard deviation of three replicate samples. *Asterisks* mark values significantly different from relevant controls (*$P < 0.05$, **$P < 0.01$, one-tailed *t* test)

at 30 min, demonstrating a slower efflux, somewhat even slower (80% residual fluorescence) in cells treated with 50 µg/ml SIL.

Silymarin interferes with cell cycle checkpoint response to doxorubicin and paclitaxel treatments

Due to reported effects of SIL on proteins engaged in cell cycle controls, we made the working hypothesis that SIL interfered with checkpoint response to DOX or TAX treatment. In order to verify the hypothesis, cell cycle distributions of single and combined treatments were evaluated by DNA flow cytometry. The experiments were made with 10 µg/ml SIL, where maximum synergistic effect was detected, and measures were made at the end of treatment. DOX treatment in LoVo caused a dose-dependent increase in $\%G_2M$, with decrease in %S, starting from 30 nM (Fig. 5a), consistent with the presence of G_1 and G_2M blocks. In combination with SIL, 30 nM DOX induced a high G_2M peak, with $\%G_2M$ reaching values in between those observed with 60 and 100 nM DOX. The cell cycle profiles of LoVo after 24-h treatment with TAX were characterised by dose-dependent increase in $\%G_2M$ and by the presence of sub-G_1 cells, indicative of an ongoing dying process (Fig. 5b). This pattern is consistent with a dose-dependent mitotic arrest accompanied with apoptosis. Addition of SIL to 30 nM TAX induced a marked increase in both G_2M and sub-G_1 cells, producing cell cycle patterns closely resembling those of samples treated with 100 nM TAX.

The same experimental protocol was applied also to LoVo/DX cells, treated with effective DOX and TAX concentrations. Cell cycle profiles of LoVo/DX treated with IC50 DOX or TAX concentrations were almost unaffected by SIL (Fig. 6).

Discussion

SIL has been reported to have anticancer activity per se and to enhance that of other anticancer drugs. At microgram/ml concentrations, SIL or silibinin induced cell cycle arrest

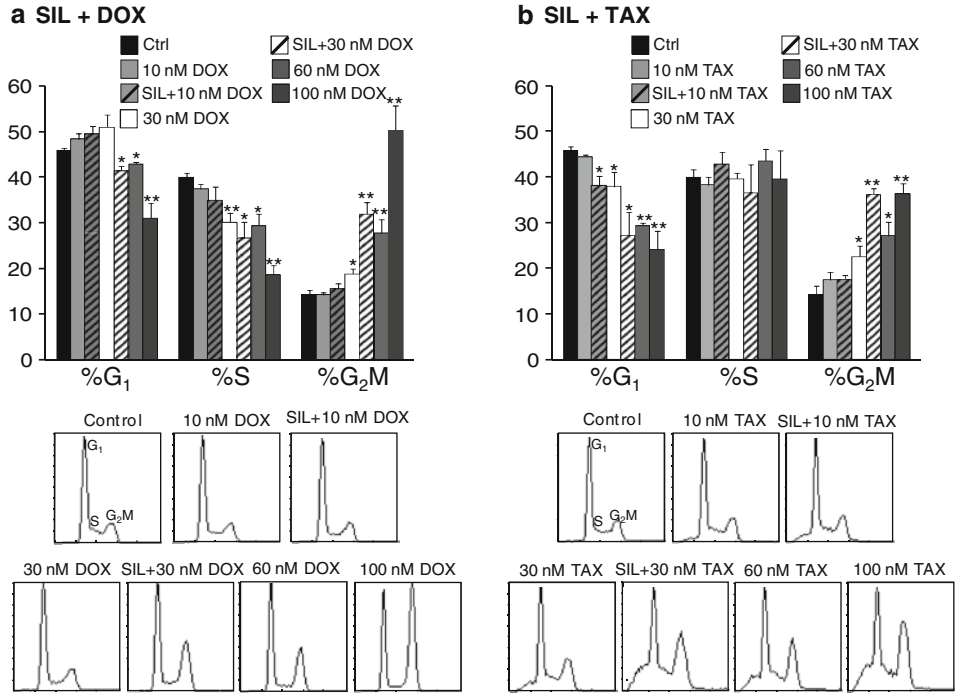

Fig. 5 Cell cycle perturbations in combined SIL-DOX and SIL-TAX treatments in LoVo. Cells were pre-treated with 10 μg/ml SIL for 24 h and then co-treated with DOX (**a**) or TAX (**b**) at the indicated concentrations. At the end of treatment, cells were harvested and analysed by DNA flow cytometry. Representative DNA histograms and bar graphs showing the mean and standard error of cell cycle percentages of three replicate samples. *Asterisks* mark values significantly different from relevant controls (*$P < 0.05$, **$P < 0.01$, two-tailed *t* test)

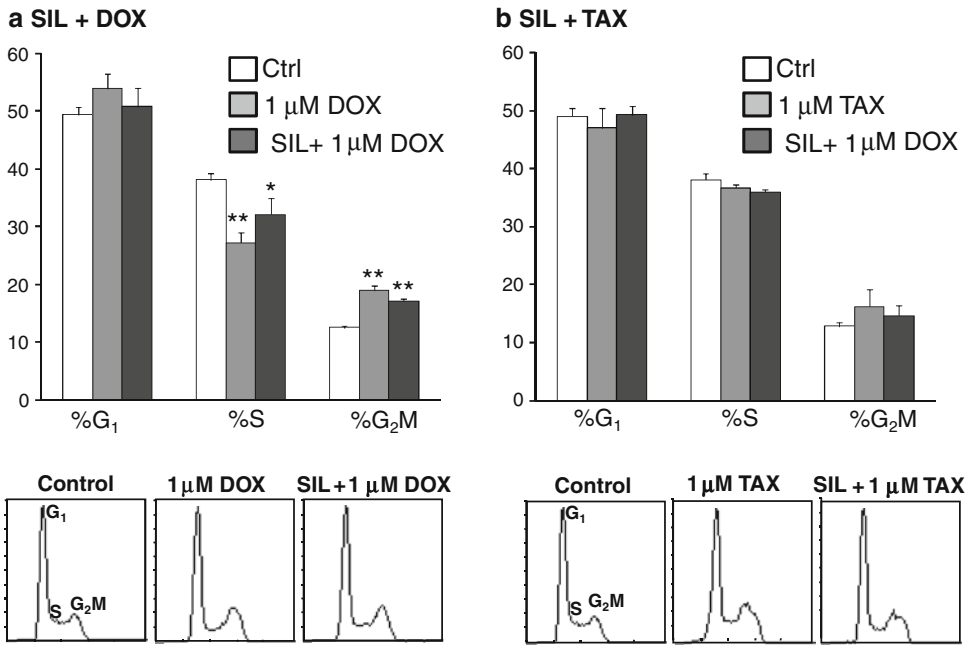

Fig. 6 Cell cycle perturbations in combined SIL-DOX and SIL-TAX treatments in LoVo/DX. Cells were pre-treated with 10 μg/ml SIL for 24 h and then co-treated with 1 μM DOX or 1 μM TAX. At the end of treatment were harvested and analysed by DNA flow cytometry. Representative DNA histograms and bar graphs showing the mean and standard error of cell cycle percentages of three replicate samples. *Asterisks* mark values significantly different from relevant controls (*$P < 0.05$, **$P < 0.01$, two-tailed *t* test)

and apoptosis in tumour cell lines in vitro, interfering with cyclin-dependent kinase (CDK) activity and other cell cycle controls [6, 36, 44]. Antiangiogenic properties were detected at concentrations even below 10 μg/ml of SIL [42, 43] and were observed also in human xenografts in mice in silibinin studies [32, 35]. In addition, SIL was reported to interact with the ATP-dependent drug-efflux pump P-gp [3, 30] and silibinin interfered with signal transduction pathways crucial to the cellular response to DNA-damaging agents [26, 32].

Recently, SIL was found active against colon cancer both in vitro and in vivo [22], but no studies have been reported on whether SIL synergises with other chemotherapeutic agents in colon cancer. The present study was designed to address this issue and evaluate the possible use of SIL to overcome MDR.

We found strong antiproliferative activity for 24-h treatment with at least 50 μg/ml SIL (Fig. 1), in LoVo. These results are consistent with previous reports of the growth inhibiting potency of silibinin in the same cell line [22], in HT-29 [1], and three other colon cancer cell lines [19] in the same concentration range. SIL was also similarly active in the MDR-resistant cell line, but a closer analysis revealed that the dynamics of cell cycle arrest was somewhat different in LoVo and LoVo/DX. In both cell lines, we found that 50 μg/ml SIL was cytostatic but not cytotoxic, as apoptosis was not detected. Cell cycle arrest was somewhat stronger in G_1 than in other phases in LoVo, and the growth-inhibitory activity did not recover immediately after drug removal, but was maintained for additional 24 h, due to a delayed crossing S and G_2M phases. This delay was not observed in LoVo/DX, showing a prompter recovery of proliferation after drug removal.

At a higher drug concentration (100 μg/ml), we detected some apoptosis in both cell lines. Cell cycle perturbation induced by SIL was less phase dependant in LoVo, with a generalised cell cycle arrest, while the same treatment produced a moderate increase in $\%G_1$ in LoVo/DX. A release of G_1 block after drug discontinuation and a more persistent G_2M block explain the accumulation of cells in G_2M in LoVo at 48 h. Instead, $\%G_2M$ did not increase significantly in LoVo/DX, but a decrease in %S indicated that G_1 block was somewhat more persistent, equally resulting in a complete growth inhibition for 24 h after drug removal. Thereafter, proliferation resumed, with similar rate in both cell lines.

SIL-DOX combinations were previously investigated in breast [37] [31], prostate [38] and lung [34] carcinomas, using silibinin in the 10–100 μM range, generally obtaining indications for a synergic effect. Silibinin did not synergize with another taxane (docetaxel) in prostate carcinoma [15]. Our study differs from the previously published ones with respect to treatment, i.e. 24-h SIL pretreatment before addition of the second drug, which was suggested by our preliminary study of SIL effects on DOX uptake. Moreover, our analysis of drug interaction explored the whole spectrum of active and sub-active concentrations of all drugs, in a factorial experimental design. We found that SIL synergized with both DOX and TAX in LoVo but not in LoVo/DX cells. SIL concentrations with low activity as single agent (10 μg/ml) performed best in combination with DOX or TAX, giving the lowest CI in LoVo, while they were additive or slightly antagonist in LoVo/DX. Instead, in LoVo/DX, we obtained the best results at higher SIL concentrations, in the range of its IC50 (50 μg/ml), with a frank additivity, without antagonism. This finding suggests the possibility of increasing the efficacy of single DOX and TAX treatments, even in resistant tumours, using SIL at growth-inhibitory concentrations. These can be reached in the colorectal mucosa in vivo not only in mice [1], but also in patients, as demonstrated by Hoh et al. [20]. Similar concentrations were also reached in plasma of patients in the phase I study of SIL [14].

We studied the origin of the drug interaction evaluating drug uptake/efflux of DOX and TAX and cell cycle perturbations in the presence of SIL. SIL was able to increase drug uptake, but at a greater extent in LoVo respect to LoVo/DX cells. The fast drug efflux characterising LoVo/DX was similarly fast in the cells co-treated with SIL, suggesting that in these cells SIL was unable to inhibit efficiently the P-gp pump, at least up to 50 μg/ml.

Nevertheless, we found that SIL did affect the drug-pumping mechanisms present in sensitive cells. Concentrations of at least 10 μg/ml were required for interaction, and SIL pre-treatment caused a significant increase in DOX and TAX uptake by LoVo cells, while in LoVo/DX DOX uptake increased modestly and TAX uptake was unaffected. Thus, when drug uptake was dominated by fast efflux caused by very high P-gp overexpression, as in LoVo/DX, SIL was poorly effective on it, vice versa it enabled to increase intracellular levels of DOX and TAX when P-gp expression was not exceedingly high and other exchange mechanism were probably relevant. Further clues on the different drug interaction of LoVo respect to Lovo/DX were provided by the cell cycle study, using the low SIL concentration, where the highest synergism had been observed. SIL at a concentration of 10 μg/ml potentiated the effects of both DOX and TAX in LoVo cells, producing cell cycle perturbations similar to those obtained with higher (more than three times) DOX and TAX concentrations. This effect was stronger than expected on the basis of the 50% uptake increase achieved with this SIL concentration, suggesting that SIL potentiated DOX and TAX activity also by other mechanisms, related to checkpoint controls and apoptosis. Instead, SIL was unable to potentiate cell cycle effects of DOX and TAX in LoVo/DX.

Different considerations should be made for 50 μg/ml and higher SIL concentrations. In this case, we observed additivity, suggesting that cell cycle delays and/or deregulations of protein expression [16] induced by SIL pretreatment might reduce the efficacy of the increased DOX or TAX uptake in LoVo. Both SIL interferences in drug uptake and cell cycle controls were possibly reduced in LoVo/DX, the balance leading again to an additive outcome.

In conclusion, our results confirm that SIL is active against colon cancer cells, at clinically achievable concentrations. The encouraging preclinical tests and the well-known low toxicity profile, reflected not only by preclinical studies [40] but also by the long safe use of silymarin in liver diseases, suggest the feasibility of developing this compound in cancer therapy, particularly exploiting a

formulation with better bioavailability [16, 21]. In a clinical perspective, it should also be noted that an increased cellular exposure to DOX produced by SIL is not expected to increase the risk of DOX-induced cardiotoxicity, because SIL was already proven to protect from such risk [11]. Thus, the SIL-DOX combination is expected to be even more efficient in terms of therapeutic index.

The present work suggests two strategies for adding SIL to current chemotherapy, both based on starting SIL before the other drugs: sensitive tumours may benefit from low SIL concentrations synergizing with standard chemotherapy, and resistant ones would benefit from the antiproliferative properties of SIL at higher concentrations, alone or in combinations with other drugs.

Acknowledgments The generous contribution of the Italian Association for Cancer Research and the Nerina and Mario Mattioli Foundation is gratefully acknowledged.

Conflict of interest statement None.

References

1. Agarwal C, Singh RP, Dhanalakshmi S, Tyagi AK, Tecklenburg M, Sclafani RA, Agarwal R (2003) Silibinin upregulates the expression of cyclin-dependent kinase inhibitors and causes cell cycle arrest and apoptosis in human colon carcinoma HT-29 cells. Oncogene 22:8271–8282
2. Cappella P, Tomasoni D, Faretta M, Lupi M, Montalenti F, Viale F, Banzato F, D'Incalci M, Ubezio P (2001) Cell cycle effects of gemcitabine. Int J Cancer 93:401–408
3. Chung SY, Sung MK, Kim NH, Jang JO, Go EJ, Lee HJ (2005) Inhibition of P-glycoprotein by natural products in human breast cancer cells. Arch Pharm Res 28:823–828
4. Colombo T, Parisi I, Zucchetti M, Sessa C, Goldhirsch A, D'Incalci M (1999) Pharmacokinetic interactions of paclitaxel, docetaxel and their vehicles with doxorubicin. Ann Oncol 10:391–395
5. D'Incalci M, Steward WP, Gescher AJ (2005) Use of cancer chemopreventive phytochemicals as antineoplastic agents. Lancet Oncol 6:899–904
6. Deep G, Singh RP, Agarwal C, Kroll DJ, Agarwal R (2006) Silymarin and silibinin cause G1 and G2-M cell cycle arrest via distinct circuitries in human prostate cancer PC3 cells: a comparison of flavanone silibinin with flavanolignan mixture silymarin. Oncogene 25:1053–1069
7. Dhanalakshmi S, Agarwal P, Glode LM, Agarwal R (2003) Silibinin sensitizes human prostate carcinoma DU145 cells to cisplatin- and carboplatin-induced growth inhibition and apoptotic death. Int J Cancer 106:699–705
8. Ding T, Tian S, Zhang Z, Gu D, Chen Y, Shi Y, Sun Z (2001) Determination of active component in silymarin by RP-LC and LC/MS. J Pharm Biomed Anal 26:155–161
9. Dolfini E, Dasdia T, Arancia G, Molinari A, Calcabrini A, Scheper RJ, Flens MJ, Gariboldi MB, Monti E (1997) Characterization of a clonal human colon adenocarcinoma line intrinsically resistant to doxorubicin. Br J Cancer 76:67–76
10. Durand RE, Olive PL (1981) Flow cytometry studies of intracellular Adriamycin in single cells in vitro. Cancer Res 41:3489–3494
11. El-Shitany NA, El-Haggar S, El-desoky K (2008) Silymarin prevents adriamycin-induced cardiotoxicity and nephrotoxicity in rats. Food Chem Toxicol 46:2422–2428
12. Enjalbert F, Rapior S, Nouguier-Soule J, Guillon S, Amouroux N, Cabot C (2002) Treatment of amatoxin poisoning: 20-year retrospective analysis. J Toxicol Clin Toxicol 40:715–757
13. Farghali H, Kamenikova L, Hynie S, Kmonickova E (2000) Silymarin effects on intracellular calcium and cytotoxicity: a study in perfused rat hepatocytes after oxidative stress injury. Pharmacol Res 41:231–237
14. Flaig TW, Gustafson DL, Su LJ, Zirrolli JA, Crighton F, Harrison GS, Pierson AS, Agarwal R, Glode LM (2007) A phase I and pharmacokinetic study of silybin-phytosome in prostate cancer patients. Invest New Drugs 25:139–146
15. Flaig TW, Su LJ, Harrison G, Agarwal R, Glode LM (2007) Silibinin synergizes with mitoxantrone to inhibit cell growth and induce apoptosis in human prostate cancer cells. Int J Cancer 120:2028–2033
16. Gallo D, Giacomelli S, Ferlini C, Raspaglio G, Apollonio P, Prislei S, Riva A, Morazzoni P, Bombardelli E, Scambia G (2003) Antitumour activity of the silybin-phosphatidylcholine complex, IdB 1016, against human ovarian cancer. Eur J Cancer 39:2403–2410
17. Grandi M, Geroni C, Giuliani FC (1986) Isolation and characterization of a human colon adenocarcinoma cell line resistant to doxorubicin. Br J Cancer 54:515–518
18. Greco WR, Bravo G, Parsons JC (1995) The search for synergy: a critical review from a response surface perspective. Pharmacol Rev 47:331–385
19. Hogan FS, Krishnegowda NK, Mikhailova M, Kahlenberg MS (2007) Flavonoid, silibinin, inhibits proliferation and promotes cell-cycle arrest of human colon cancer. J Surg Res 143:58–65
20. Hoh C, Boocock D, Marczylo T, Singh R, Berry DP, Dennison AR, Hemingway D, Miller A, West K, Euden S, Garcea G, Farmer PB, Steward WP, Gescher AJ (2006) Pilot study of oral silibinin, a putative chemopreventive agent, in colorectal cancer patients: silibinin levels in plasma, colorectum, and liver and their pharmacodynamic consequences. Clin Cancer Res 12:2944–2950
21. Kaur M, Agarwal R (2007) Silymarin and epithelial cancer chemoprevention: how close we are to bedside? Toxicol Appl Pharmacol 224:350–359
22. Kaur M, Velmurugan B, Tyagi A, Deep G, Katiyar S, Agarwal C, Agarwal R (2009) Silibinin suppresses growth and induces apoptotic death of human colorectal carcinoma LoVo cells in culture and tumor xenograft. Mol Cancer Ther 8:2366–2374
23. Krishan A, Ganapathi R (1980) Laser flow cytometric studies on the intracellular fluorescence of anthracyclines. Cancer Res 40:3895–3900
24. Lee JI, Hsu BH, Wu D, Barrett JS (2006) Separation and characterization of silybin, isosilybin, silydianin and silychristin in milk thistle extract by liquid chromatography-electrospray tandem mass spectrometry. J Chromatogr A 1116:57–68
25. Letteron P, Labbe G, Degott C, Berson A, Fromenty B, Delaforge M, Larrey D, Pessayre D (1990) Mechanism for the protective effects of silymarin against carbon tetrachloride-induced lipid peroxidation and hepatotoxicity in mice. Evidence that silymarin acts both as an inhibitor of metabolic activation and as a chain-breaking antioxidant. Biochem Pharmacol 39:2027–2034
26. Lin CJ, Sukarieh R, Pelletier J (2009) Silibinin inhibits translation initiation: implications for anticancer therapy. Mol Cancer Ther 8:1606–1612
27. Loewe S, Muischenek H (1926) Effect of combinations: mathematical basis of the problem. Arch Exp Pathol Pharmakol 114:313–326

28. Lupi M, Matera G, Branduardi D, D'Incalci M, Ubezio P (2004) Cytostatic and cytotoxic effects of topotecan decoded by a novel mathematical simulation approach. Cancer Res 64:2825–2832
29. Meschini S, Calcabrini A, Monti E, Del Bufalo D, Stringaro A, Dolfini E, Arancia G (2000) Intracellular P-glycoprotein expression is associated with the intrinsic multidrug resistance phenotype in human colon adenocarcinoma cells. Int J Cancer 87:615–628
30. Morris ME, Zhang S (2006) Flavonoid-drug interactions: effects of flavonoids on ABC transporters. Life Sci 78:2116–2130
31. Scambia G, De Vincenzo R, Ranelletti FO, Panici PB, Ferrandina G, D'Agostino G, Fattorossi A, Bombardelli E, Mancuso S (1996) Antiproliferative effect of silybin on gynaecological malignancies: synergism with cisplatin and doxorubicin. Eur J Cancer 32A:877–882
32. Singh RP, Dhanalakshmi S, Agarwal C, Agarwal R (2005) Silibinin strongly inhibits growth and survival of human endothelial cells via cell cycle arrest and downregulation of survivin, Akt and NF-kappaB: implications for angioprevention and antiangiogenic therapy. Oncogene 24:1188–1202
33. Singh RP, Gu M, Agarwal R (2008) Silibinin inhibits colorectal cancer growth by inhibiting tumor cell proliferation and angiogenesis. Cancer Res 68:2043–2050
34. Singh RP, Mallikarjuna GU, Sharma G, Dhanalakshmi S, Tyagi AK, Chan DC, Agarwal C, Agarwal R (2004) Oral silibinin inhibits lung tumor growth in athymic nude mice and forms a novel chemocombination with doxorubicin targeting nuclear factor kappaB-mediated inducible chemoresistance. Clin Cancer Res 10:8641–8647
35. Singh RP, Sharma G, Dhanalakshmi S, Agarwal C, Agarwal R (2003) Suppression of advanced human prostate tumor growth in athymic mice by silibinin feeding is associated with reduced cell proliferation, increased apoptosis, and inhibition of angiogenesis. Cancer Epidemiol Biomarkers Prev 12:933–939
36. Tyagi A, Agarwal C, Harrison G, Glode LM, Agarwal R (2004) Silibinin causes cell cycle arrest and apoptosis in human bladder transitional cell carcinoma cells by regulating CDKI-CDK-cyclin cascade, and caspase 3 and PARP cleavages. Carcinogenesis 25:1711–1720
37. Tyagi AK, Agarwal C, Chan DC, Agarwal R (2004) Synergistic anti-cancer effects of silibinin with conventional cytotoxic agents doxorubicin, cisplatin and carboplatin against human breast carcinoma MCF-7 and MDA-MB468 cells. Oncol Rep 11:493–499
38. Tyagi AK, Singh RP, Agarwal C, Chan DC, Agarwal R (2002) Silibinin strongly synergizes human prostate carcinoma DU145 cells to doxorubicin-induced growth Inhibition, G2-M arrest, and apoptosis. Clin Cancer Res 8:3512–3519
39. Ubezio P (1985) Microcomputer experience in analysis of flow cytometric DNA distributions. Comput Programs Biomed 19:159–166
40. Vogel G, Trost W, Braatz R, Odenthal KP, Brusewitz G, Antweiler H, Seeger R (1975) Pharmacodynamics, site and mechanism of action of silymarin, the antihepatoxic principle from Silybum mar. (L) Gaertn. 1. Acute toxicology or tolerance, general and specific (liver-) pharmacology. Arzneimittelforschung 25:82–89
41. Willey TA, Bekos EJ, Gaver RC, Duncan GF, Tay LK, Beijnen JH, Farmen RH (1993) High-performance liquid chromatographic procedure for the quantitative determination of paclitaxel (Taxol) in human plasma. J Chromatogr 621:231–238
42. Yang SH, Lin JK, Chen WS, Chiu JH (2003) Anti-angiogenic effect of silymarin on colon cancer LoVo cell line. J Surg Res 113:133–138
43. Yang SH, Lin JK, Huang CJ, Chen WS, Li SY, Chiu JH (2005) Silibinin inhibits angiogenesis via Flt-1, but not KDR, receptor up-regulation. J Surg Res 128:140–146
44. Zi X, Grasso AW, Kung HJ, Agarwal R (1998) A flavonoid antioxidant, silymarin, inhibits activation of erbB1 signaling and induces cyclin-dependent kinase inhibitors, G1 arrest, and anticarcinogenic effects in human prostate carcinoma DU145 cells. Cancer Res 58:1920–1929